Syntheses of Oligophenylenevinylenes−Polyisoprene Diblock Copolymers and Their Microphase Separation

Wenjie Li, Henbin Wang, and Luping Yu*

Department of Chemistry and The James Franck Institute, The University of Chicago, 5735 South Ellis Avenue, Chicago, Illinois 60637

Terry L. Morkved and Henrich M. Jaeger

Department of Physics and The James Frank Institute, The University of Chicago, 5640 South Ellis Avenue, Chicago, Illinois 60637

Received October 27, 1998

ABSTRACT: A series of functionalized oligophenylenevinylene (OPV) molecules have been synthesized via an orthogonal approach for the purpose of preparing diblock copolymers. The coupling reaction between the aldehyde-terminated OPVs and a "living" polyisoprene (PI) species leads to the formation of OPV−PI diblock copolymers. TEM results on thin films of four copolymers with the same OPV block but different lengths of the PI blocks clearly show nanophase separation. Alternating strips of OPV- and PI-rich lamella domains were observed under TEM, confirmed by the SAXS experiments on bulk samples. Temperature-dependent SAXS studies also revealed an order−disorder transition at around 128 °C for copolymer **1**, which is consistent with the TEM results.

Conjugated polymers are known to possess interesting electrical and optical properties, such as high electric conductivity upon doping, large third-order optical nonlinearity, and electroluminescence properties.[1−3] Since conjugated polymers possess rigid backbones, diblock copolymers containing conjugated blocks may exhibit a unique microphase separation behavior due to their self-assembling property. Thus, it is possible to obtain one-, two-, or three-dimensional confinements of the conjugated domains. These structures could offer an opportunity to study quantum confinement effects, tunneling effects in carrier transport, and the phase transition phenomenon.[4−6] Such structures may also lead to novel electronic, optoelectronic, and optical properties not found in conjugated homopolymers.[7]

In the past, there were several attempts at synthesizing and characterizing diblock copolymers containing π-conjugated blocks.[8−15] Most cases had limited success in obtaining nanophase separation morphologies. Cohen et al.[12] were able to synthesize diblock copolymers containing a π-conjugated block. Microphase separation of different morphologies in six of these copolymers (and their precursor polymers) were observed. More recently, Jenekhe et al. reported the synthesis of poly(phenylquinoline)−polystyrene diblock copolymers which self-assembled into various morphologies.[16] Meijer et al. reported the synthesis of a polystyrene−oligothiophene−polystyrene triblock copolymer and observed a spherical domain structure.[17]

In 1996, our group developed a two-stage approach for synthesizing novel diblock copolymers containing a π-conjugated block.[18] The first stage involved the synthesis of a conjugated block with a well-defined molecular weight and proper functionality which could be used in the second stage for coupling with a living polymer species to form the desired diblock copolymer. An oligo(3-alkylthiophene)−polystyrene diblock copolymer system was synthesized, but no phase separation was observed, as indicated by TEM studies.

Earlier theoretical work predicted that the product of the Flory−Huggins segment−segment interaction parameter χ and the total degree of polymerization of the diblock N is $\chi N = 10.5$ at the minimum of the phase diagram boundary.[19,20] Below this value, the diblock copolymer will exist in a homogeneous state. Therefore, in order for phase separation to occur in this system, both the χ parameter and N value have to be increased. To increase the χ value, one can increase the structural difference between the two types of monomers and the solubility parameter difference between the two block segments.[21] To achieve a larger N value, a longer conjugated block is needed.

On the basis of these considerations, we succeeded in synthesizing another diblock copolymer system consisting of olio(phenylenevinylene) (OPV) and polyisoprene. We chose this system for several reasons. First of all, the structural difference between the blocks of this system is much larger than that of the oligothiophene−polystyrene diblock copolymers. For example, the solubility parameters for various polymer repeat units present in the diblock copolymers can be estimated by group contribution methods developed by Van Krevelen.[22] The calculated values are as follows: polystyrene, 19.1; oligo(3-hexylthiophene), 18.7; polyisoprene, 17.4; oligo(alkyl-substituted phenylenevinylene), 19.6; all with units of $J^{1/2}/cm^{3/2}$. The difference in the oligothiophene−polystyrene system is 0.4 and 2.2 in the OPV−polyisoprene system; thus, a larger χ value between the two blocks in the OPV−polyisoprene system can be expected. Also, a longer oligo(phenylenevinylene) block, which will increase the N value, can be synthesized. Larger χ and N values will eventually make microphase separation possible in this system. Second, polyisoprene can be selectively stained by osmium tetraoxide (OsO_4) to produce amplitude contrast between the two blocks

10.1021/ma981679i CCC: $18.00
Published on Web 04/09/1999

Scheme 1. Synthesis of the OPV Building Blocks

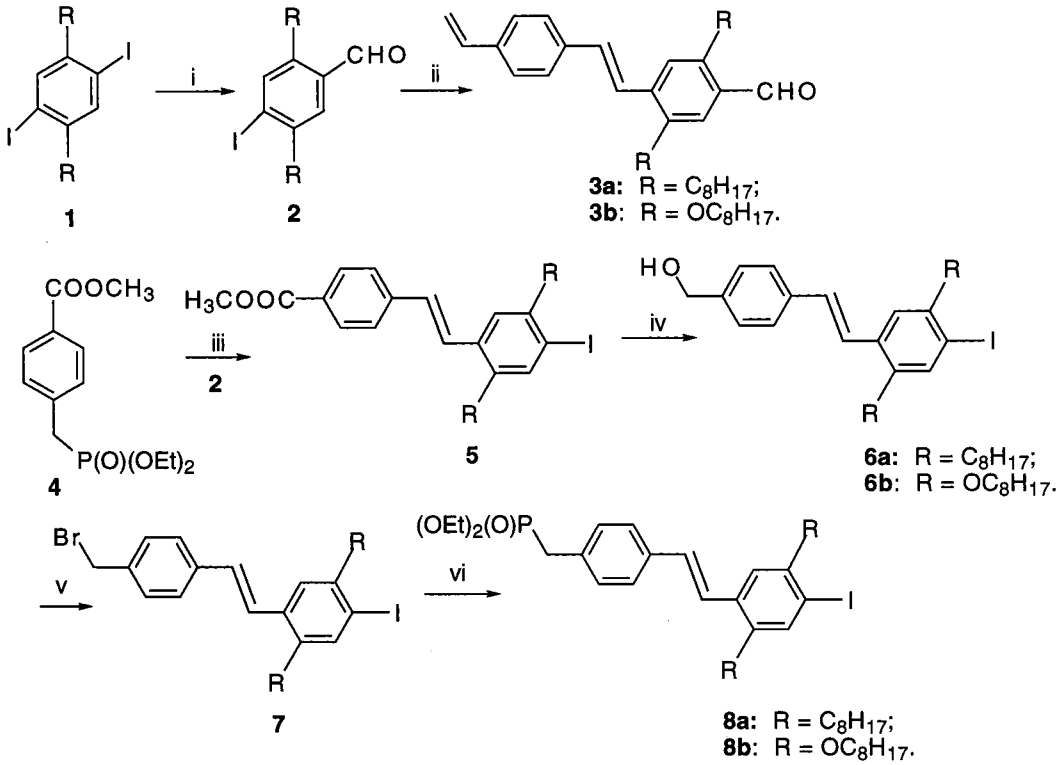

Reaction Conditions: i. n-BuLi//DMF; ii. p-Divinylbenzene, $Pd(OAc)_2$, Bu_3N, $P(o\text{-Tolyl})_3$; iii. NaH; iv. $LiAlH_4$; v. PBr_3; vi. $P(OEt)_3$

R = C_8H_{17} or OC_8H_{17}.

under TEM so that microphase separation can be more easily detected. Furthermore, OPV molecules with precisely controlled molecular length, size, and shape can serve as model systems for understanding the relationships between bulk material properties and molecular structures in their polydispersed analogues: poly(phenylenevinylene)s.

To synthesize the OPV block with defined molecular length, we developed a general strategy that utilizes two types of reactions to grow the conjugated chain stepwise, without the need for protecting group chemistry. The end-functionalized OPVs were further coupled with living polyisoprene species to form diblock copolymers with a conjugated block.[18] As expected, our experimental results demonstrated nanophase separation in this system. This paper describes the synthesis of the OPV molecules, their diblock copolymers, and the microphase separation behavior of these copolymers.

Results and Discussion

Synthesis of Functionalized OPVs and Their Diblock Copolymers. In a previous publication, we described an orthogonal approach (alternative application of two reactions: the Horner−Wadsworth−Emmons reaction and the Heck reaction) to the synthesis of the end-functionalized OPVs with alkoxy side chains.[23] Schemes 1 and 2 show our approach for the synthesis of OPV with alkyl side chains. The strategy outlined here is identical to those described previously.[23] Two building block molecules, compounds **3** and **8**, possess mutually complementary functional ends and were synthesized according to Scheme **1**. The aldehyde group on compound **3** will react with the phosphonate ester terminus of compound **8** via the Horner−Wadsworth−Emmons reaction to form a carbon−carbon double bond. The iodo substituent at one end of compound **8** can couple with the vinyl terminus of compound **3** under the Heck reaction conditions to form a carbon−carbon single bond. The sequential and alternating addition of these two building blocks in growing an OPV chain leads to the formation of OPVs with either one-end or double-end functionality. In this paper, we describe only the mono-end functionalized OPV and corresponding diblock copolymers.

The purified OPVs produced from this approach have an all-trans structure. A detectable amount of cis product (less than 5%) was generated in the Horner−Wadsworth−Emmons reaction, and a few regioisomers were observed in the Heck reaction. These side products were separated by flash chromatography using a mixture of hexane and chloroform as the eluent.[24−26] The longest OPV synthesized by this approach is compound **16**, which has 14 aryl rings and 13 double bonds and a molecular weight of 3117.

To prepare diblock copolymers, we used the carbon−carbon bond formation between the living anionic polyisoprene species and an aldehyde group. Polyisoprene species of different chain lengths were generated by a living polymerization fashion using Li(*sec*-Bu) as an initiator (Scheme 3). The excess OPV aldehydes were then removed by flash chromatography using a mixture of hexane and chloroform as the eluent. The resulting diblock copolymers are quite soluble in most organic

Scheme 2. Synthesis of Functionalized OPVs

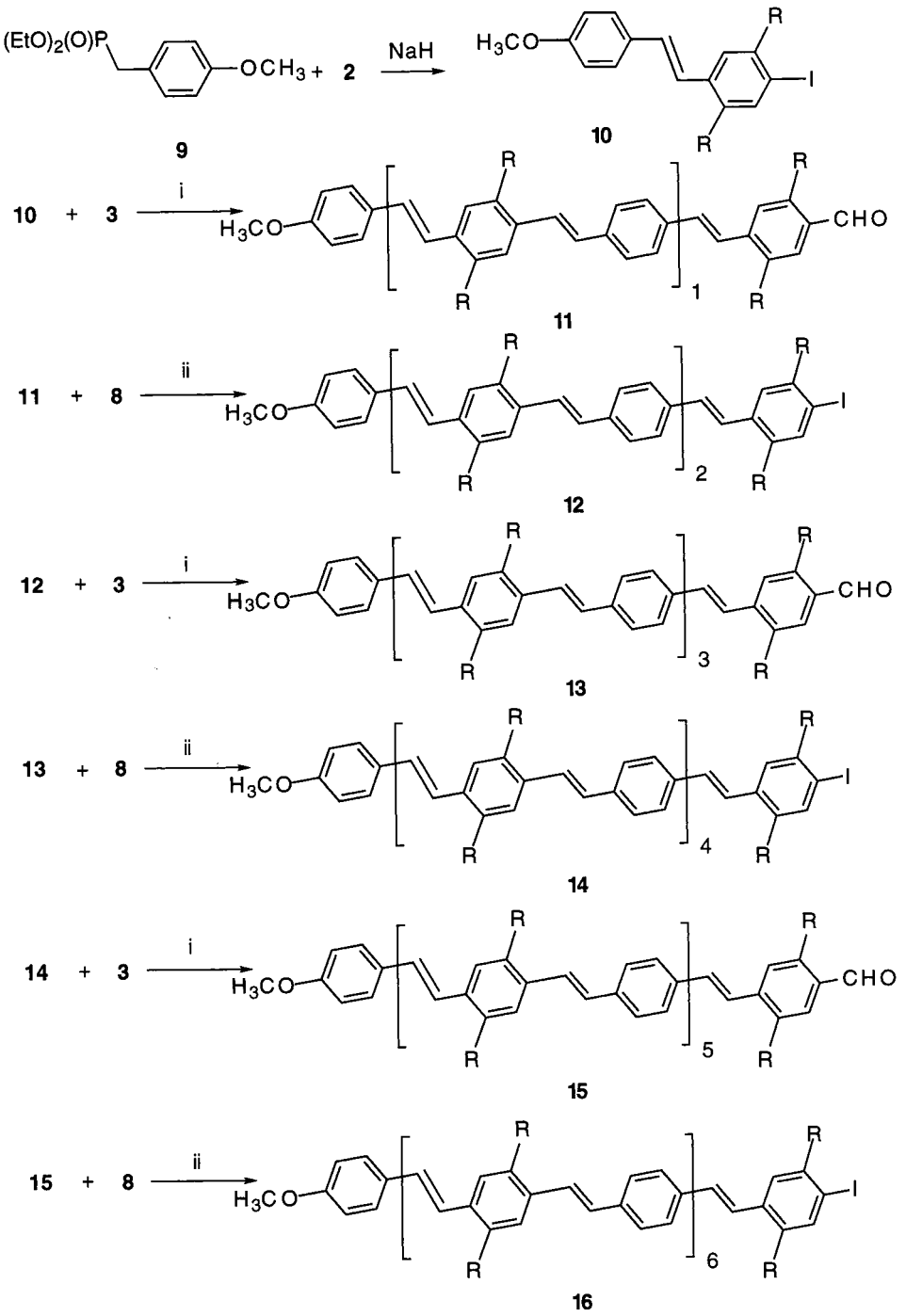

Reaction Conditions: i. $Pd(OAc)_2$, $P(o\text{-}tolyl)_3$, Bu_3N. ii. NaH.

Key: Compound serie **a**: R = C_8H_{17}; **b**: R = OC_8H_{17}.

solvents. The syntheses for each diblock copolymer with a certain molecular weight were reproducible.

Structural Characterization. The structures of the end-functionalized OPVs were studied by using ^{1}H NMR, mass spectrometry, and combustion analysis. The ^{1}H NMR spectra of the longer OPVs are complicated. However, several characteristic peaks can be assigned. For example, in the ^{1}H NMR spectrum of the longest OPV compound **16a**, the chemical shift of aromatic proton ortho to the iodo functional appears at 7.62 ppm. The chemical shift of the terminal methyl group appears at 2.38 ppm, and those of methylene protons adjacent to the phenyl rings are found at 2.77 ppm. The ^{1}H NMR spectrum of the OPV with aldehyde functionality (compound **15b**) shows a chemical shift due to the aldehyde proton at 10.45 ppm. The matrix-assisted laser desorption ionization (MALDI) mass spectrum of compound **15b** supports its structural assignments. A molecular ion peak of $[M + H]^+$ at $m/z = 2783.1 \pm 2.7$ was found, which is very close to the calculated value of $m/z = 2781.0$.

The molecular weights and polydispersity of these diblock copolymers were characterized by an on-line GPC light scattering setup using THF as the eluent.

Scheme 3. Synthesis of the Diblock Copolymers

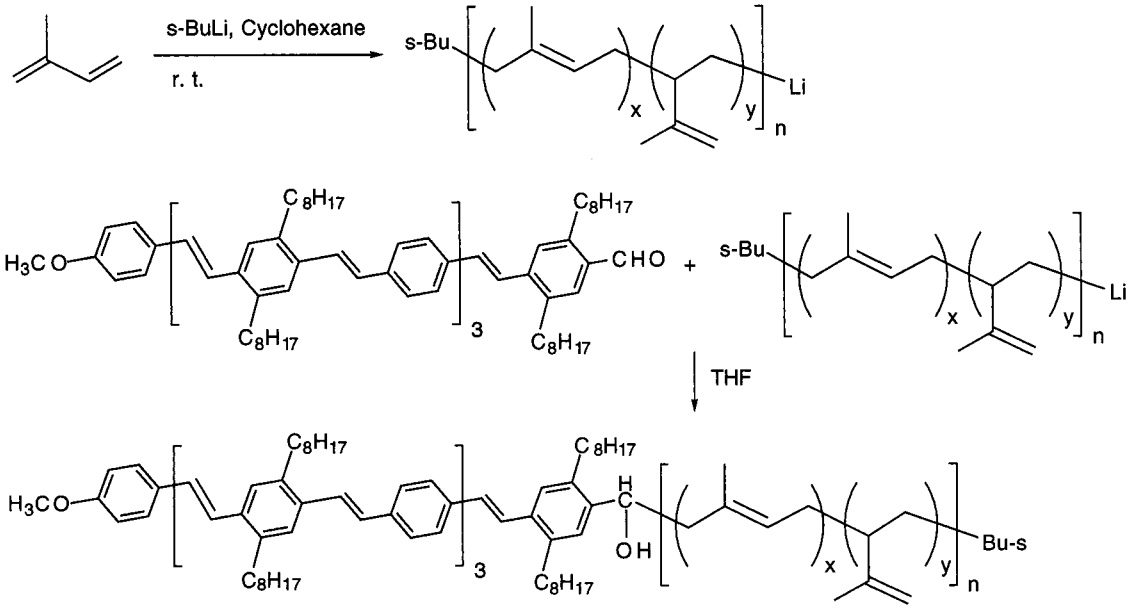

Copolymers **1 - 4**

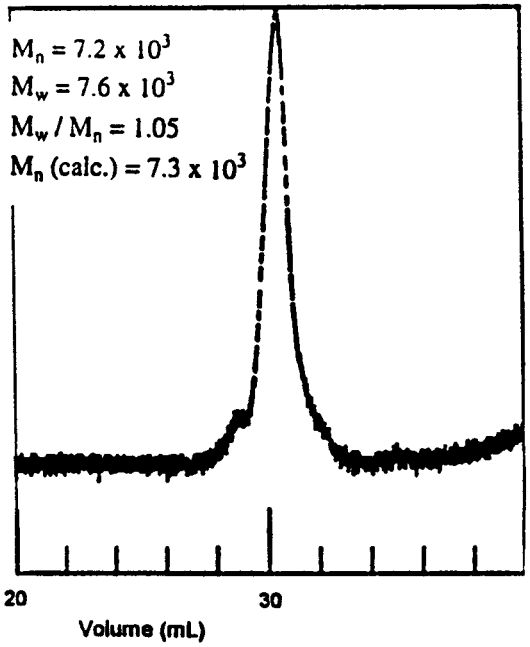

Figure 1. GPC light scattering profile of copolymer **2**.

Table 1. GPC Light Scattering Results of Copolymers

polymer	M_n	M_w/M_n	W_{OPV}[a]	T_m (°C)[b]	T_c (°C)[c]
copolymer **1**	4400	1.08	0.40	105	129
copolymer **2**	7200	1.05	0.24	95	108
copolymer **3**	8400	1.08	0.21	82	104
copolymer **4**	14400	1.04	0.12	78	94

[a] Weight fraction of OPV block. [b] Crystal−nematic transition temperature. [c] Clearing temperature.

The GPC light scattering profile of copolymer **2** is shown in Figure 1. The measured number-averaged molecular weight is 7.2×10^3, which is very close to the calculated value of 7.3×10^3. All of the copolymers have relatively narrow polydispersities (Table 1). The weight fractions of the OPV block in the diblock copolymers were calculated from the GPC light scattering results, ranging from 0.40 (copolymer **1)** to 0.12 (copolymer **4)** (Table 1).

The polyisoprene blocks consist of 91−93% of the structural units formed by 1,4 addition and 7−9% by 3,4 addition, as estimated by FTIR[27] and ^{1}H NMR[28] spectra of the copolymers. In the FTIR spectrum of copolymer **1**, the C−H bending mode from the 1,4 linkages in the polyisoprene appears to be a broad band at 838 cm^{-1}. The C−H bending mode of the isopropenyl groups arising from 3,4 addition can be found at 888 cm^{-1}.[27] In the ^{1}H NMR spectra of the copolymers, the vinyl proton corresponding to the 1,4 addition appears at 5.1 ppm. The isopropenyl protons from 3,4 addition are at 4.7 ppm.

All of the OPVs have strong and broad absorptions in the visible region. The absorption of the octoxy-substituted OPVs is red-shifted compared to those of the corresponding octyl-substituted OPVs because of the electronic effect and lesser steric hindrance of octoxy groups. For both octyl- and octoxy-substituted OPVs, the absorption maxima increase as the conjugation length increases. For example, a red shift of 29 nm was observed when the conjugation length increased from compound **11a** to compound **16a** (Figure 2a). However, the saturation in absorption maxima is observed after the conjugation length reaches eight benzene rings and seven double bonds. A similar trend was observed for the octoxy-substituted OPV series (Table 2). The saturation in absorption maximum due to the limited electron delocalization in longer oligomers has been described previously in the literature.[29] The fact that the absorption maxima of these molecules converge to that of the corresponding polymers over relatively short conjugation lengths suggests the validity of using these OPVs as model compounds for the study of the electronic properties of PPV materials. The extinction coefficients of the absorption spectra of these OPVs increase with the conjugation length because the oscillator strength of these molecules increases as the conjugation length-ens.

Table 2. Spectroscopic Data and Termal Transition Temperatures of OPVs[a]

	11		12		13		14		15		16
	a	b	a	b	a	b	a	b	a	b	a
λ_{max}[b] (nm)	392	431	405	441	414	457	419	460	421	463	421
λ_{max}[c] (nm)	498	527	469	497	480	511	480	514	482	518	481
			498	529	409	543	510	545	511	548	511
Φ[d] (%)	60	45	57	54	48	53	57	59	58	56	61
T_m[e] (°C)	113	97	130	67	145	90	150	113	165	105	170
T_c[f] (°C)	NA[g]	NA	140	87	170	113	186	176	200	185	203

[a] a: R = C_8H_{17}; b: R = OC_8H_{17}. [b] Absorption maxima. [c] Fluorescence maxima. [d] Fluorescence quantum yield. [e] Crystal−nematic transition temperature. [f] Clearing temperature. [g] NA = not applicable.

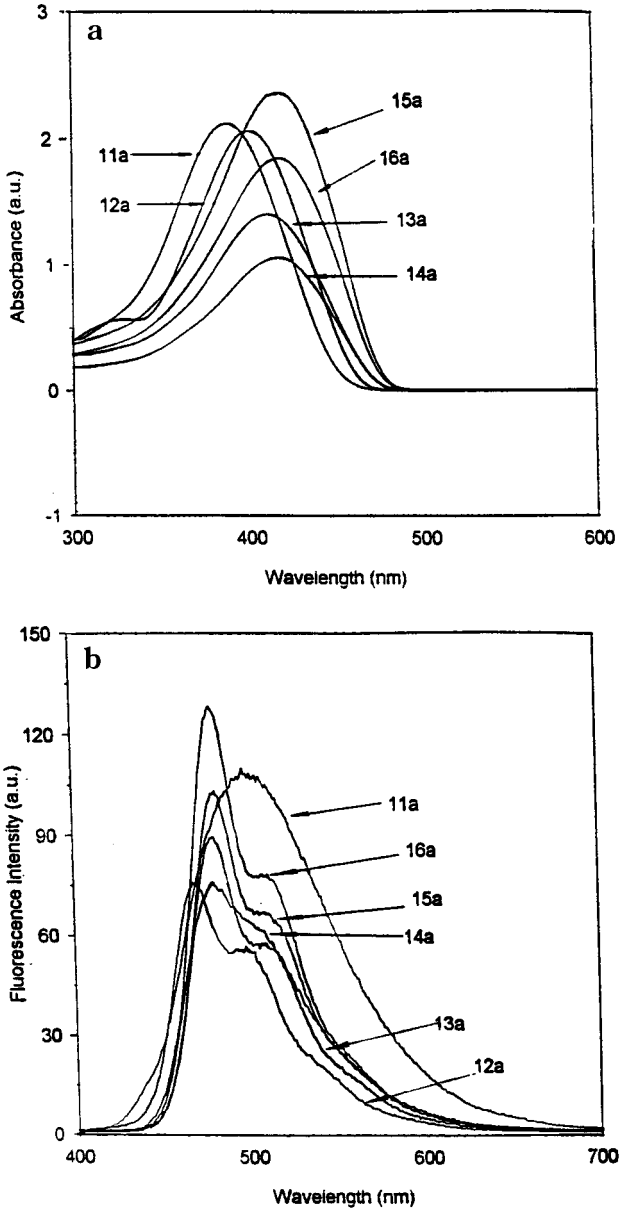

Figure 2. (a) UV/vis spectra of dioctyl-substituted OPVs. (b) Fluorescence spectra of dioctyl-substituted OPVs.

Solutions of these oligomers give a brilliant green fluorescence (Figure 2b). Except the shortest oligomers **11a** and **11b**, each of the OPVs exhibit three main bands in its fluorescence spectrum, typical of the emission patterns for PPV.[30] The emission spectra of compounds **11a** and **11b** are very broad and show none of the fine features present in the other spectra. The fluorescent quantum yields of these OPVs are sizable, ranging from 0.5 to 0.7. No clear trends were observed as the conjugation length increases.

Figure 3. Polarizing micrograph of liquid-crystalline texture of compound **13b** at 138 °C. The magnification is 400 times.

Thermal Properties. These OPVs are "hairy rod" molecules and show a reversible thermotropic liquid-crystalline transition.[31,32] The thermal transition temperatures of all of the OPVs are listed in Table 2. The liquid-crystalline texture observed by using a polarizing microscope shows a typical Schlieren pattern which is evidence for the presence of nematic phases (Figure 3). The crystal−nematic transition point (T_m) and clearing temperature (T_c) show a rough correlation with the conjugation length: both the T_m and the T_c increase as the conjugation length increases. The temperature range of the liquid-crystalline phase also becomes broader with increasing conjugation length. The alkyl-substituted OPVs exhibit a higher melting point and clearing temperature than their corresponding alkoxy-substituted analogues.

Thermal properties of the copolymers were investigated by DSC and TGA measurements. DSC studies indicated that each copolymer has two types of thermal transitions: one may correspond to the crystal−nematic transition temperature (T_m) ranging from 82 °C (copolymer **4)** to 104 °C (copolymer **1)**, and another corresponds to liquid-crystal clearing temperature ranging from 94 °C (copolymer **4)** to 129 °C (copolymer **1**) (see Table 1). The T_m and T_c decrease as the weight fraction of the OPV block decreases. These thermal transitions and the liquid-crystal state of the diblock copolymers were observed by a polarized microscope. Small-angle X-ray scattering studies described in later sections also revealed a LC−isotropic transition. TGA studies revealed that these copolymers are stable up to 330 °C.

Microphase Separation Behaviors of Diblock Copolymers. The microphase separation behaviors of copolymers **1**−**4** were studied by using TEM and SAXS. Copolymers **1**−**4** have the same block lengths of OPV

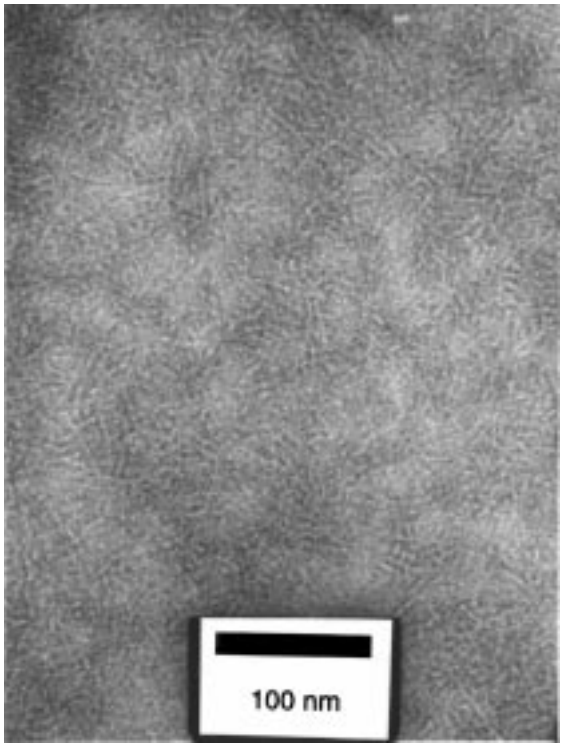

Figure 4. TEM micrograph of copolymer **1** before annealing.

but different lengths of the PI block. For TEM studies, thin films on amorphous silicon nitride substrates were prepared by spin-casting the copolymer solutions in toluene. The film thicknesses were controlled by varying spinning speed and copolymer concentration. Generally, a spinning speed of 3000 rpm and a concentration of 1 wt % give a film thickness of 50−70 nm as determined by ellipsometry. After being stained with OsO_4 vapor, these films show nanophase separation in the as-cast state. OsO_4 preferentially stains the unsaturated bonds of the polyisoprene (PI) block, creating contrast between OPV and PI blocks. As shown in Figure 4a, the microstructure of copolymer **1** consists of OPV-rich (light) and PI-rich (dark) strips. The strips are arranged randomly and occasionally intersect with other strips. They have lengths from 20 to 100 nm. The average widths of the strips are 6−7 nm for OPV-rich domains and 5−6 nm for PI-rich domains. Similar microstructures were obtained for other copolymers (Figure 4b,c).

After they were annealed at temperatures above their melting points, these copolymer films showed periodic structures of OPV and PI domains. Dewetting of the copolymer film on the substrate was observed after annealing, which caused an increase in the actual film thickness compared with the as-cast ones. Shown in Figure 5 are TEM micrographs of copolymers **1**−**4** after annealing at 120 °C for 15 h. All four samples showed alternating OPV- and PI-rich strips. The average widths of these strips are shown in Figure 6. The OPV-rich strips have an average domain spacing of ∼6 nm in all four samples. The domain spacing of the PI strips increases with the molecular weight of the PI block in the copolymers and ranges from ∼5 nm in copolymer **1** to ∼13 nm in copolymer **4**. Annealing these films at higher temperatures (above 135 °C) led to the disappearance of the microphase-separated structures. These results indicate that the order−disorder transition temperatures (T_{ODT}) in these copolymers are lower than 135 °C. On the other hand, varying annealing times from 6 to 120 h at 120 °C did not noticeably change the morphologies.

Similar morphologies were also observed on thin film samples of these copolymers prepared by casting dilute solutions in cyclohexane (0.05 wt %) onto carbon-coated mica sheets in a solvent-saturated atmosphere. The solvent was allowed to evaporate in a period of approximately 2 h. The thin carbon-supported films were held under a vacuum for a day before being floated off on distilled water and picked up on copper grids. Samples were stained with OsO_4 vapor before being examined by TEM. Shown in Figure 7 is the TEM micrograph of copolymer **2** on carbon-supported films. The repeat spacing for OPV and PI blocks is consistent with the results from silicon nitride supported films. It is known that the solvent concentration could affect the Flory−Huggins interaction parameter χ between the two blocks in a copolymer system, but increasing copolymer concentration via solvent evaporation causes an increase in χ value and eventually leads to microphase separation from the isotropic state.

The morphologies of these copolymers resemble lamella microstructures of coil−coil diblock copolymers that are oriented perpendicular to the substrates. Normally, lamellae are observed for coil−coil diblock copolymers in which both blocks occupy nearly equal volume fractions. Early theoretical studies on microphase separation behavior of rod−coil diblocks by Semenov and Vasilenko predicted monolayer and bilayer lamella structures as well as tilted lamellae.[33,34] Lamella morphologies have been observed experimentally in rod−coil diblock copolymers with a polypeptide as the rod block.[31−34] For example, Gallot et al. studied the phase separation of polybutadiene−poly(benzyl-L-glutamate), polybutadiene−poly(N^5-hydroxypropylglutamine), polystyrene−poly(carbobenzoxy-L-lysine), and polybutadiene−poly(carbobenzoxy-L-lysine) using TEM and SAXS.[35,36] By changing the polypeptide concentration from 18% to 75%, they found that the structures of the mesophases are always lamellae, at least within their experimental concentration range.

We suggest that the microphase structures of our copolymers are also lamella. Further evidence for the lamella morphology comes from the SAXS experiment in which the phase behavior in bulk materials was studied. Figure 8 shows the SAXS patterns obtained from a bulk sample of copolymer **1** at different temperatures. The sample was first annealed at 150 °C for 10 min to reach a disordered state and then allowed to cool slowly to room temperature. The diffraction pattern at 20 °C consists of two Bragg reflections appearing at reciprocal space position ratios of 1 and 2, indicating a lamella microstructure (Figure 8a). The second-order reflection is relatively small and broad, which suggests this material is weakly segregated as supported by the absence of higher-order reflections. From the positions of the two reflections, a repeat spacing of 167 ± 1 Å was estimated through the equation $d = 2\pi/q$ for bulk copolymer **1** sample at 20 °C. This value is larger than the repeat spacing (∼100 Å) obtained for thin films of copolymer **1** from TEM experiments. This discrepancy can be easily understood because the TEM images show only the contrast exposed to the surface. The measured thickness is not the real thickness of the layers but rather a projection of the true thickness to the surface. The thickness from TEM measurements are therefore

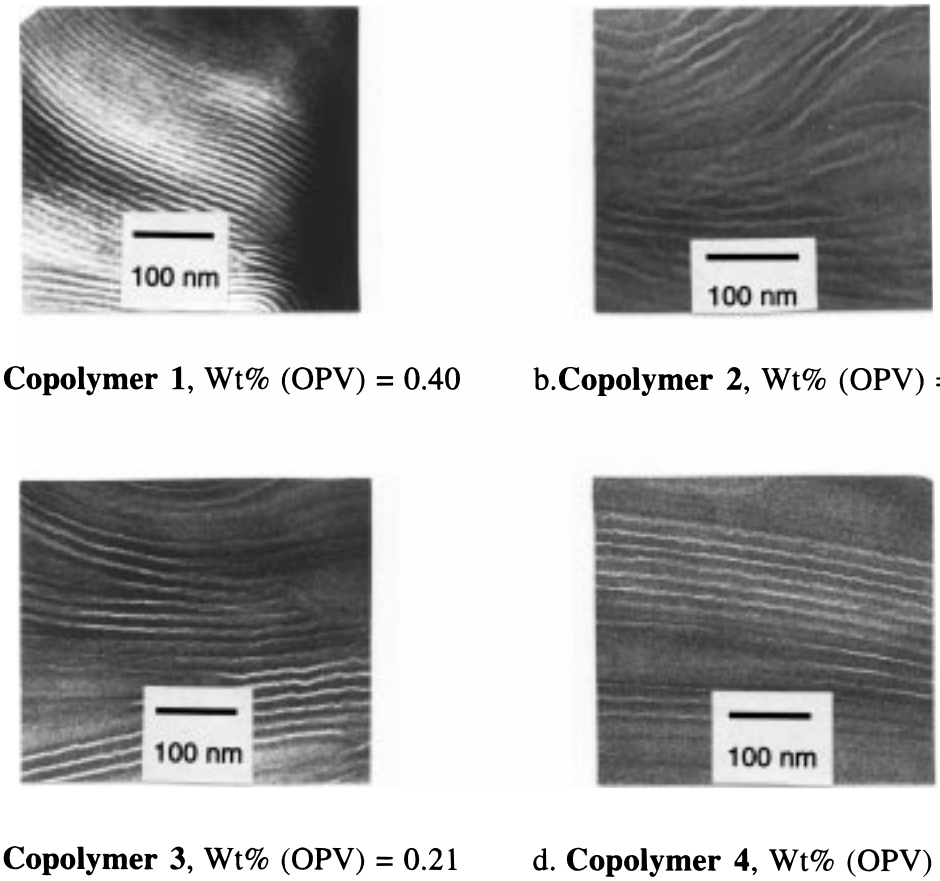

a. **Copolymer 1**, Wt% (OPV) = 0.40 b.**Copolymer 2**, Wt% (OPV) = 0.24

c. **Copolymer 3**, Wt% (OPV) = 0.21 d. **Copolymer 4**, Wt% (OPV) = 0.12

Figure 5. TEM micrographs of copolymers **1**−**4** after annealing at 120 °C for 15 h: (a) copolymer **1**; (b) copolymer **2**; (c) copolymer **3**; (d) copolymer **4**.

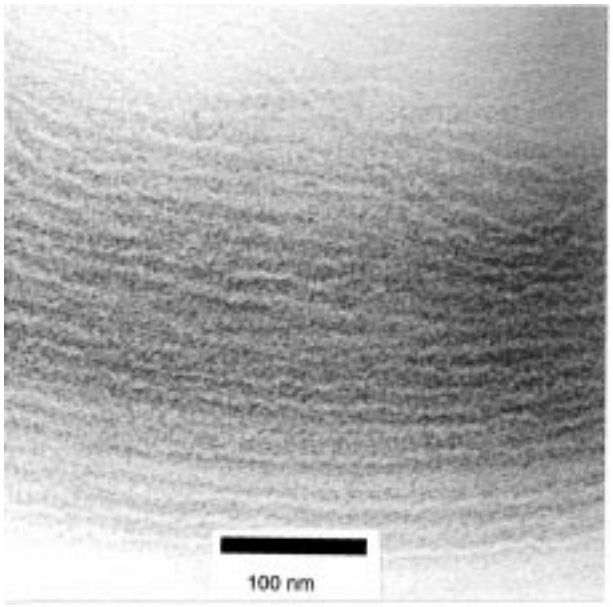

Figure 6. TEM micrograph of copolymer **2** on carbon-supported films.

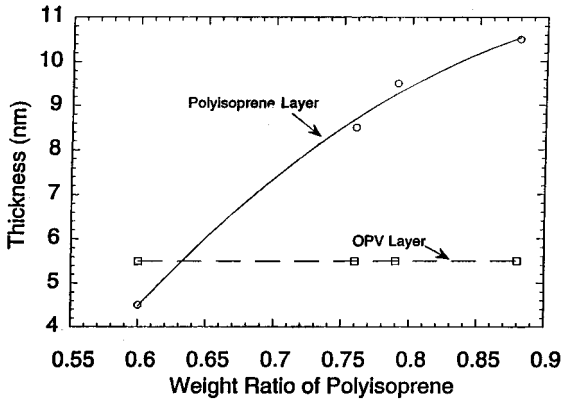

Figure 7. Average widths of OPV layers and PI layers as a function of composition.

underestimated, and a thickness measurement obtained from SAXS is more reliable. Since the length of the conjugated block was estimated to be ~5.2 nm and the widths of the OPV-rich domains in all four copolymers remain constant, the microstructures might be double-layer lamella (Scheme 4). In this structure, the OPV block layers possess a thickness of 10 nm and those of polyisoprene of ca. 6−7 nm. A similar SAXS pattern was observed with copolymer **4** with a repeat spacing of 295 ± 1 Å. This result further supports the bilayer structure for these nanophases.

Reheating the bulk sample of copolymer **1** from 20 to 100 °C causes little change in the lamella structure (Figure 8b). However, when the temperature reaches 120 °C, the intensities of both reflections start to decrease (Figure 8c). The two reflection peaks eventually disappear after the sample is heated above 128 ± 2 °C, which signals the T_{ODT} of bulk copolymer **1** sample. This supports the observation of T_{ODT} in thin-film samples. The successive cooling from the disordered state gives a reversible process of the heating stages, which further confirms the existence of the lamella structure in the bulk samples (Figure 8e−h).

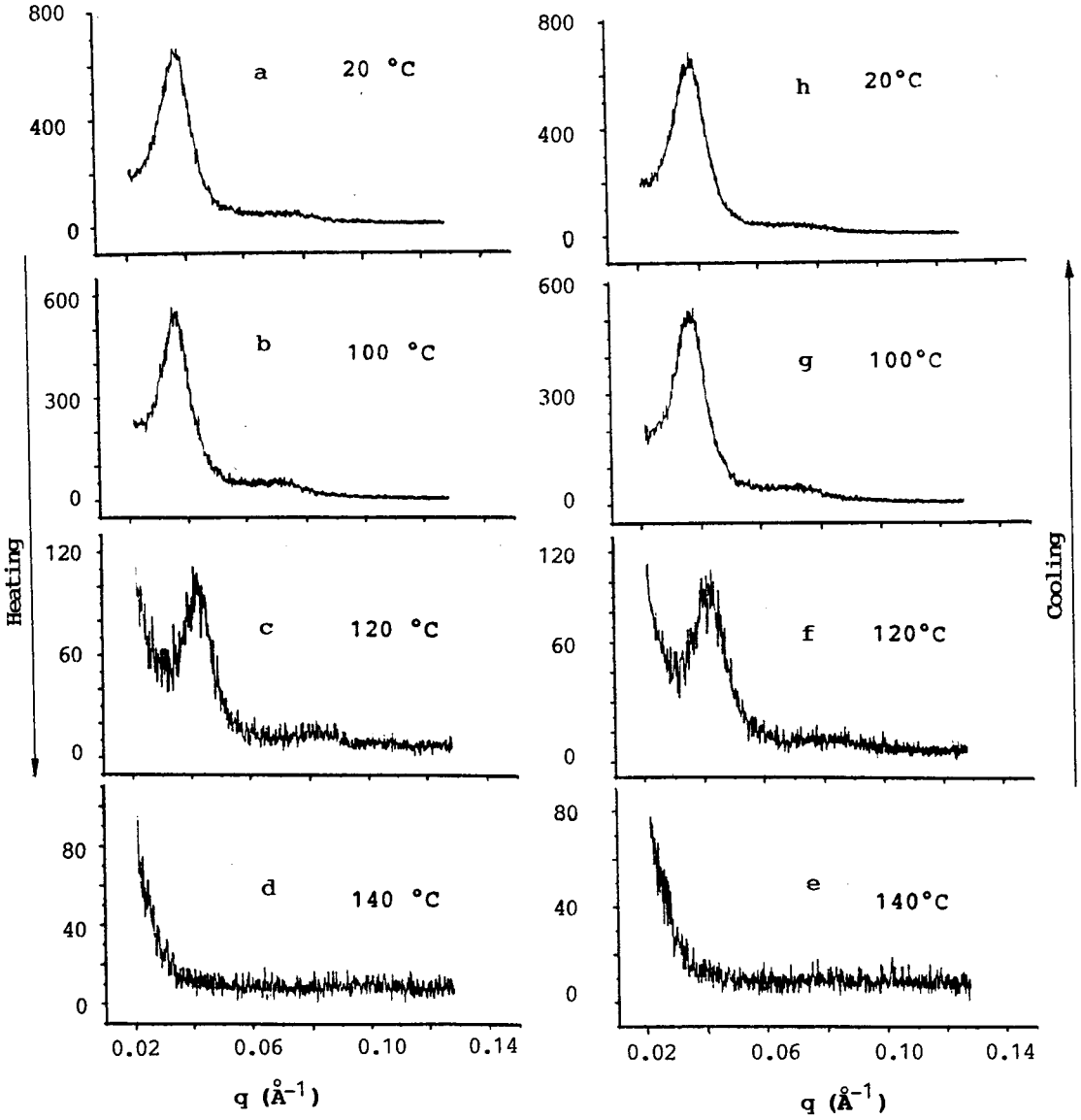

Figure 8. SAXS profiles for copolymer **1**: (a)−(d) heating stages; (e)−(h) cooling stages.

The SAXS results seem to suggest that the diblock copolymer might be thermotropic since the disappearance of the reflection peaks at higher temperatures above T_{ODT} is quite different from the experimental results reported on amorphous coil−coil diblock copolymers, in which only a discontinuous change in peak intensity was observed across the ODT.[37−39] Mortensen et al. recently reported a similar finding on a low molecular weight diblock copolymer of poly(ethylene oxide) (PEO) and polystyrene studied by small-angle neutron scattering (SANS).[40] They ascribed the total disappearance of the correlation peak to the melting of the crystalline PEO block at T_{ODT}, which results in a lack of contrast between the two types of polymer blocks under SANS. In our copolymer system, the OPV block has a liquid-crystalline window from 145 to 170 °C in its pure state. The copolymerization of the OPV block with polyisoprene could lower both its melting point and clearing temperature since the polyisoprene block acts as plasticizer. Therefore, the disappearance of the reflection peaks at T_{ODT} could also be due to the phase transition from crystalline to LC state of the OPV block in the copolymer system, which drags the PI blocks into the OPV domain and decreases the electron density difference between the OPV and PI blocks.

Scheme 4. Bilayer Structure of the Lammella Phase of the Copolymers

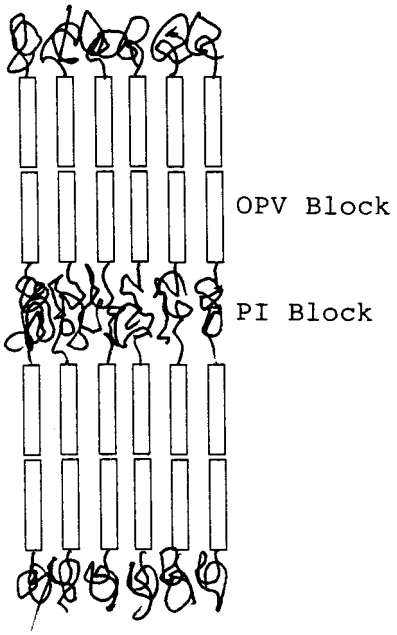

Conclusions

An orthogonal approach to the stepwise synthesis of long, functionalized OPV molecules has been developed. These OPV molecules exhibited high fluorescence quantum yields and a reversible thermotropic liquid-crystalline phase. The coupling reaction between the aldehyde-terminated OPVs and a "living" polyisoprene species leads to the formation of diblock copolymers. Four copolymers that have the same OPV block but different lengths of the PI block were synthesized. TEM results on thin-film samples clearly show that these copolymers could undergo microphase separation and form periodic structures. Alternating strips of OPV- and PI-rich domains were observed under TEM. The domain sizes of the strips suggest that these microstructures could be bilayer lamella phases predicted by Semenov and Vasilenko.[33,34] The lamellar structure of the copolymer with the shortest polyisoprene block was further confirmed by the SAXS experiment on bulk samples. SAXS studies also reveal that this copolymer has an order−disorder transition at around 128 °C, which is consistent with the TEM results.

These nanophase patterns of OPV block copolymers would be very interesting to study further. It is known that conjugated polymers are usually mixtures of macromolecules of different molecular weights, and they are extremely difficult to recrystallize. Therefore, many physical measurements are simply the statistical average results. These self-assembled domains bring these OPV molecules into order and hence the opportunity to study the intrinsic physical properties of conjugated polymers.

Experimental Section

Materials. 1,4-Diiodo-2,5-dioctylbenzene (**1a**),[31] 1,4-diiodo-2,5-dioctoxybenzene (**1b**),[31] *p*-divinylbenzene,[32] and 4-(diethoxyphosphorylmethyl)benzoic acid methyl ester (**4**)[41] were prepared according to literature procedures. Tetrahydrofuran (THF) was redistilled from Na^+/benzophenone ketyl. Cyclohexane was purified according to ref 42. Isoprene was redistilled under argon and dried over calcium hydride before use. All of the other chemicals were purchased from the Aldrich Chemical Co. and used as received unless otherwise stated.

Synthesis of OPV Building Blocks. Compound 2a. In a flask purged with nitrogen 1,4-diiodo-2,5-dioctylbenzene (**1a**) (37.7 g, 68 mmol) was dissolved in 200 mL of dry ethyl ether. The mixture was stirred at room temperature. A solution of *n*-Buli (27.2 mL of 2.5 M in hexanes, 68 mmol) diluted with 30 mL of ether was added dropwise over a period of 1.5 h via an additional funnel. The mixture was stirred for an additional 0.5 h, and then DMF (5.6 mL, 71 mmol) was added all at once. The resulting solution was stirred at room temperature for 2 h. A 100 mL aliquot of 1 M H_3PO_4 was added. The mixture was partitioned, and the organic phase was washed with water three times. The organic layer was dried over $MgSO_4$ and concentrated by rotary evaporation. The crude product was further purified by flash chromatography (silica gel, hexane/ethyl acetate (20/1)) to give 25 g of white solid (80% yield). ^{1}H NMR ($CDCl_3$, ppm): δ 10.22 (s, 1 H), 7.75 (s, 1 H), 7.59 (s, 1 H), 2.90 (t, 2 H), 2.72 (t, 2 H), 1.58 (m, 4 H), 1.28 (m, 20 H), 0.88 (m, 6 H).

Compound 2b. It was obtained from compound **1b** in 75% yield, following a similar procedure as described for compound **2a**. ^{1}H NMR ($CDCl_3$, ppm): δ 10.34 (s, 1 H), 7.40 (s, 1 H), 7.13 (s, 1 H), 3.98 (m, 4 H), 1.80 (m, 4 H), 1.47 (m, 4 H), 1.30 (m, 16 H), 0.88 (m, 6 H).

Compound 3a. In a two-necked round-bottom flask was added *p*-divinylbenzene (6.6 g, 50.8 mmol), tri-*o*-tolyphosphene (1.1 g, 3.6 mmol), NBu_3 (11.1 g, 60 mmol), and $Pd(OAC)_2$ (162 mg, 0.72 mmol). The stirring mixture was heated to 80 °C, and then a solution of compound **2a** (10.9 g, 24 mmol) in 20 mL of DMF was added. The resulting mixture was stirred under reflux for 24 h. The reaction solution was then cooled to room temperature and diluted with 100 mL of Et_2O. Water was added, and the organic layer was separated and washed with water three times. The organic layer was dried over $MgSO_4$ and concentrated to give a yellow/orange oil. The oil was purified by a silica gel chromatography column using hexane as the eluent first to remove the unreacted *p*-divinylbenzene and then hexane/ethyl acetate (100/2) as the eluent to give 7.64 g of yellow solid (72% yield). ^{1}H NMR ($CDCl_3$, ppm): δ 10.24 (s, 1 H), 7.64 (s, 1 H), 7.51 (d, J = 8.3 Hz, 2 H), 7.48 (s, 1 H), 7.44 (d, J = 8.3 Hz, 2 H), 7.34 (d, J = 16.1 Hz, 1 H), 7.11 (d, J = 16.1 Hz, 1 H), 6.73 (dd, 1 H), 5.79 (d, J = 17.6 Hz, 1 H), 5.28 (d, J = 11.0 Hz, 1 H), 3.01 (t, 2 H), 2.77 (t, 2 H), 1.56 (m, 4 H), 1.27 (m, 20 H), 0.88 (m, 6 H). Anal. Calcd for $C_{33}H_{46}O$: C, 86.40; H, 10.11. Found: C, 86.51; H, 10.13.

Compound 3b. It was obtained from compound **2b** in 65% yield, following a similar procedure as described for compound **3a**. ^{1}H NMR ($CDCl_3$, ppm): δ 10.37 (s, 1 H), 7.45 (d, J = 7.95 Hz, 2 H), 7.41 (d, J = 16.4 Hz, 1 H), 7.36 (d, J = 7.90 Hz, 2 H), 7.27 (s, 1 H), 7.17 (d, J = 16.4 Hz, 1 H), 7.12 (s, 1 H), 6.68 (dd, 1 H), 5.74 (d, J = 17.6 Hz, 1 H), 5.23 (d, J = 10.9 Hz, 1 H), 4.08 (t, 2 H), 4.01 (t, 2 H), 1.84 (m, 4 H), 1.49 (m, 4 H), 1.29 (m, 16 H), 0.89 (m, 6 H). Anal. Calcd for $C_{33}H_{46}O_3$: C, 80.75; H, 9.47. Found: C, 80.81; H, 9.43.

Compound 5a. In a two-necked round-bottom flask was added compound **4** (10.9 g, 38.1 mmol), sodium hydride (0.92 g, 38.1 mmol), and 20 mL of DME. The mixture was brought to reflux. A solution of compound **2a** (15.8 g, 34.7 mmol) in 15 mL of DME was then added dropwise through an additional funnel. When TLC indicated that the aldehyde was consumed, the mixture was cooled to room temperature and diluted with 50 mL of ethyl ether. Water was added, and the organic layer was separated and washed with water three times. The organic layer was dried over $MgSO_4$ and concentrated by rotary evaporation. The crude product was further purified by flash chromatography (silica gel, hexane/ethyl acetate (10/1)) to give 17.6 g of light yellow solid (86% yield). ^{1}H NMR ($CDCl_3$, ppm): δ 8.05 (d, J = 8.3 Hz, 2 H), 7.63 (s, 1 H), 7.55 (d, J = 8.3 Hz, 2 H), 7.40 (s, 1 H), 7.36 (d, J = 16.2 Hz, 1 H), 7.01 (d, J = 16.1 Hz, 1 H), 3.93 (s, 3 H), 2.67 (m, 4 H), 1.59 (m, 4 H), 1.29 (m, 20 H), 0.89 (m, 6 H).

Compound 6a. In a two-necked round-bottom flask was added compound **5a** (15.5 g 26.3 mmol) and 50 mL of dry ethyl ether. The mixture was cooled to 0 °C by an ice bath. $LiAlH_4$ (650 mg, 17 mmol) was then added in small portions, and vigorous bubbling of the solution occurred. After 0.5 h the ice bath was removed, and the mixture was allowed to warm to room temperature for an additional 0.5 h. The mixture was diluted with ether (100 mL). A 50 mL aliquot of 1 M HCl was added. The organic layer was separated and washed with water (3 × 45 mL). The organic layer was dried over $MgSO_4$ and concentrated to give 14.6 g of light yellow liquid (>95% yield). ^{1}H NMR ($CDCl_3$, ppm): δ 7.61 (s, 1 H), 7.51 (d, J = 8.1 Hz, 2 H), 7.40 (s, 1 H), 7.37 (d, J = 8.1 Hz, 2 H), 7.25 (d, J = 16.1 Hz, 1 H), 6.99 (d, J = 16.1 Hz, 1 H), 4.71 (s, 2 H), 2.66 (m, 4 H), 1.58 (m, 4 H), 1.29 (m, 20 H), 0.89 (m, 6 H).

Compound 7a. Compound **6a** (14.6 g, 26.1 mmol) was dissolved in 60 mL of dry ethyl ether. The mixture was cooled to 0 °C. Phosphorus tribromide (4.25 g, 15.7 mmol) was added slowly via a syringe to the above mixture. The resulting was stirred at 0 °C for 1 h. Excess PBr_3 was quenched by the slow addition of methanol. The mixture was then diluted with 50 mL of Et_2O and poured into water. The organic layer was separated and washed with saturated $NaHCO_3$ (1 × 30 mL), water (2 × 30 mL), and brine (2 × 30 mL). The organic layer was dried over $MgSO_4$ and concentrated by rotary evaporation. The product was further purified by flash chromatography (silica gel, hexane) to give 13.5 g of light yellow solid (85%, yield). ^{1}H NMR ($CDCl_3$, ppm): δ 7.55 (s, 1 H), 7.41 (d, 2 H), 7.32 (m, 3 H), 7.21 (d, 1 H), 6.92 (d, 1 H), 4.48 (s, 2 H), 2.66 (t, 2 H), 2.61 (t, 2 H), 1.56 (m, 4 H), 1.28 (m, 20 H), 0.88 (m, 6 H).

Compound 7b. It was obtained from compound **5b** in 60% yield, following a similar procedure as described from com-

pound **5a** to compound **7a**. ^{1}H NMR ($CDCl_3$, ppm): δ 7.42 (d, 2 H), 7.32 (m, 3 H), 7.23 (s, 1 H), 7.05 (d, 1 H), 6.95 (s, 1 H), 4.48 (s, 2 H), 3.98 (t, 2 H), 3.92 (t, 2 H), 1.82 (m, 4 H), 1.49 (m, 4 H), 1.29 (m, 16 H), 0.88 (m, 6 H).

Compound 8a. In a round-bottom flask were added compound **7a** (13.3 g, 21.3 mmol) and triethyl phosphite (7.07 g, 42.6 mmol). The resulting mixture was heated to reflux for 10 h. After the reaction was completed, the excess triethyl phosphite was removed by vacuum distillation. The product was purified by flash chromatography (silica gel, hexane/ethyl acetate (3/2)) to give 13.3 g of light yellow solid (92%, yield). ^{1}H NMR ($CDCl_3$, ppm): δ 7.61 (s, 1 H), 7.45 (d, J = 7.95 Hz, 2 H), 7.39 (s, 1 H), 7.30 (dd, 2 H), 7.23 (d, J = 16.4 Hz, 1 H), 6.96 (d, J = 16.1 Hz, 1 H), 4.04 (m, 4 H), 3.16 (d, 2 H), 2.66 (m, 4 H), 1.58 (m, 4 H), 1.27 (m, 26 H), 0.89 (m, 6 H). Anal. Calcd for $C_{35}H_{54}IO_3P$: C, 61.76; H, 8.00. Found: C, 61.91; H, 7.96.

Compound 8b. It was obtained from compound **7b** in 90% yield, following a similar procedure as described for compound **8a**. ^{1}H NMR ($CDCl_3$, ppm): δ 7.40 (d, 2 H), 7.30 (d, 1 H), 7.23 (m, 3 H), 7.04 (d, 1 H), 6.96 (s, 1 H), 3.98 (m, 6 H), 3.92 (t, 2 H), 3.13 (d, 2 H), 1.81 (m, 4 H), 1.55 (m, 4 H), 1.25 (m, 22 H), 0.88 (m, 6 H). Anal. Calcd for $C_{35}H_{54}IO_5P$: C, 58.97; H, 7.65; I, 17.80. Found: C, 59.09; H, 7.69; I, 17.91.

Synthesis of Functionalized OPVs: **General Procedure for the Wittig Reaction.** Compound **8** and the aldehyde-terminated OPV were dissolved in a mixture of NMP and THF. After the mixture was heated to reflux about 1.2 equiv of NaH was added, the resulting solution was stirred under reflux for 5 h. Water and methanol were added, and the precipitate was collected by suction filtration and washed with water and methanol (or acetone in the case of longer OPVs) several times. The product was further purified by flash chromatography using a mixture of hexane and chloroform as the eluent to give a yellow to orange solid, depending upon the molecular weight. The eluent needed to be heated for longer OPVs purification.

Compound 10a. ^{1}H NMR ($CDCl_3$, ppm): δ 7.60 (s, 1 H), 7.39 (m, 3 H), 7.19 (m, 3 H), 6.96 (d, 1 H), 2.65 (m, 4 H), 2.37 (s, 3 H), 1.58 (m, 4 H), 1.27 (20 H), 0.88 (m, 6 H).

Compound 10b. ^{1}H NMR ($CDCl_3$, ppm): δ 7.35 (d, J = 7.8 HZ, 2 H), 7.27 (d, J = 16.4 Hz, 1 H), 7.22 (s, 1 H), 7.10 (d, J = 7.7 Hz, 2 H), 7.03 (d, J = 16.4 Hz, 1 H), 6.96 (s, 1 H), 3.98 (t, 2 H), 3.91 (t, 2 H), 2.34 (s, 3 H), 1.81 (m, 4 H), 1.52 (m, 4 H), 1.29 (m, 16 H), 0.88 (m, 6 H).

Compound 12a. ^{1}H NMR ($CDCl_3$, ppm): δ 7.62 (s, 1 H, aromatic H), 7.54 (s, 8 H, aromatic H), 7.46−7.42 (m, 7 H, aromatic H), 7.41−7.28 (m, 4 H, olefinic H), 7.19 (d, 2 H, aromatic H), 7.11−6.98 (m, 6 H, olefinic H), 2.77 (m, 12 H), 2.38 (s, 3 H), 1.65 (br, 12 H), 1.29 (br, 60 H), 0.88 (m, 18 H). Anal. Calcd for $C_{95}H_{133}I$: C, 81.39; H, 9.56. Found: C, 81.47; H, 9.61.

Compound 12b. ^{1}H NMR ($CDCl_3$, ppm): δ 7.47 (m, 8 H), 7.44−7.36 (m, 7 H), 7.33 (s, 1 H), 7.23 (s, 1 H), 7.12−7.05 (m, 10 H), 6.98 (s. 1 H), 4.04 (m, 10 H), 3.93 (t, 2 H), 2.35 (s, 3 H), 1.86 (m, 12 H), 1.53 (m, 12 H), 1.30 (m, 48 H), 0.89 (m, 18 H). Anal. Calcd for $C_{95}H_{133}IO_6$: C, 76.26; H, 8.84; I, 8.48. Found: C, 76.19; H, 8.86; I, 8.64. MS: m/z, 1497.0 (M^+).

Compound 14a. ^{1}H NMR ($CDCl_3$, ppm): δ 7.62 (s, 1 H, aromatic H), 7.54 (br, 16 H, aromatic H), 7.46−7.42 (m, 11 H, aromatic H), 7.41−7.28 (m, 8 H, olefinic H), 7.19 (d, 2 H, aromatic H), 7.11−6.98 (m, 10 H, olefinic H), 2.77 (m, 20 H), 2.38 (s, 3 H), 1.65 (m, 20 H), 1.29 (br, 100 H), 0.89 (m, 30 H). Anal. Calcd for $C_{159}H_{221}I$: C, 84.52; H, 9.86. Found: C, 84.27; H, 9.84.

Compound 14b. ^{1}H NMR ($CDCl_3$, ppm): 7.47−7.43 (m, 20 H), 7.38−7.36 (dd, 3 H), 7.33 (s, 1 H), 7.23 (s, 1 H), 7.12−7.05 (m, 22 H), 6.98 (s. 1 H), 4.04 (m, 18 H), 3.93 (t, 2 H), 2.35 (s, 3 H), 1.86 (m, 20 H), 1.53 (m, 20 H), 1.30 (m, 80 H), 0.89 (m, 30 H). Anal. Calcd for $C_{159}H_{221}IO_{10}$: C, 78.93; H, 9.23; I, 5.25. Found: C, 79.06; H, 9.20; I, 5.42. MS: m/z, 2420.5 ($(M + H)^+$).

Compound 16a. ^{1}H NMR ($CDCl_3$, ppm): δ 7.62 (s, 1 H, aromatic H), 7.54 (br, 24 H, aromatic H), 7.46−7.42 (m, 15 H, aromatic H), 7.41−7.28 (m, 12 H, olefinic H), 7.19 (d, 2 H, aromatic H), 7.11−6.98 (m, 14 H, olefinic H), 2.77 (m, 28 H), 2.38 (s, 3 H), 1.65 (m, 28 H), 1.29 (br, 140 H), 0.89 (m, 42 H). Anal. Calcd for $C_{223}H_{309}I$: C, 85.94; H, 9.99. Found: C, 86.06; H, 10.08.

General Procedure for the Heck Reaction. Compound **3**, iodo-terminated OPV, POT, and tributylamine were added to a two-necked round-bottom flask along with a mixture of NMP and THF as the solvent. The mixture was heated to 90 °C. When all reagents dissolved, the $Pd(OAc)_2$ was added, and the resulting mixture was then stirred at 100 °C for 8 h. The reaction mixture was cooled to room temperature. Water and methanol were added. The precipitate was collected by suction filtration and was washed with water and methanol (or acetone in the case of longer OPVs) several times. The product was further purified by flash chromatography using a mixture of hexane and chloroform as the eluent to give a yellow to orange solid, depending upon the molecular weight. The eluent needed to be heated for longer OPVs purification.

Compound 11a. ^{1}H NMR ($CDCl_3$, ppm): δ 10.26 (s, 1 H), 7.66 (s, 1 H, aromatic H), 7.56 (s, 4 H, aromatic H), 7.51 (s, 1 H, aromatic H), 7.45−7.43 (m, 4 H, aromatic H), 7.41−7.29 (m, 3 H, olefinic H), 7.20 (d, 2 H, aromatic H), 7.15 (d, 1 H, olefinic H), 7.05 (d, 1 H, olefinic H), 7.02 (d, 1 H, olefinic H), 3.03 (t, 2 H), 2.77 (m, 6 H), 2.39 (s, 3 H), 1.64 (m, 8 H), 1.29 (m, 40 H), 0.89 (m, 12 H). Anal. Calcd for $C_{64}H_{90}O$: C, 87.81; H, 10.36. Found: C, 87.62; H, 10.25.

Compound 11b. ^{1}H NMR ($CDCl_3$, ppm): δ 10.37 (s, 1 H), 7.48 (s, 4 H, aromatic H), 7.44 (s, 1 H, aromatic H), 7.43 (d, 1 H, olefinic H), 7.39−7.36 (dd, 3 H, 2 aromatic H, 1 olefinic H), 7.28 (s, 1 H, aromatic H), 7.19 (d, 1 H, olefinic H), 7.13−7.05 (m, 6 H, 3 aromatic H, 3 olefinic H), 4.09 (t, 2 H), 4.03 (m, 6 H), 2.35 (s, 3 H), 1.85 (m, 8 H), 1.51 (m, 8 H), 1.30 (m, 32 H), 0.88 (m, 12 H). Anal. Calcd for $C_{64}H_{90}O_5$: C, 81.81; H, 9.67. Found: C, 81.89; H, 9.63. MS: m/z, 939.2 (M^+).

Compound 13a. ^{1}H NMR ($CDCl_3$, ppm): δ 10.26 (s, 1 H), 7.66 (s, 1 H, aromatic H), 7.56 (br, 12 H, aromatic H), 7.51 (s, 1 H, aromatic H), 7.46−7.43 (m, 8 H, aromatic H), 7.42−7.29 (m, 6 H, olefinic H), 7.20 (d, 2 H, aromatic H), 7.18−7.01 (m, 8 H, olefinic H), 3.03 (t, 2 H), 2.77 (m, 14 H), 2.39 (s, 3 H), 1.64 (m, 16 H), 1.29 (m, 80 H), 0.89 (m, 24 H). Anal. Calcd for $C_{128}H_{178}O$: C, 88.72; H, 10.35. Found: C, 88.57; H, 10.29.

Compound 13b. ^{1}H NMR ($CDCl_3$, ppm): δ 10.37 (s, 1 H), 7.48−7.43 (m, 18 H), 7.39−7.36 (dd, 3 H), 7.28 (s, 1 H), 7.13−7.05 (m, 16 H), 4.09 (t, 2 H), 4.03 (m, 14 H), 2.35 (s, 3 H), 1.85 (m, 16 H), 1.51 (m, 16 H), 1.30 (m, 64 H), 0.88 (m, 24 H). Anal. Calcd for $C_{128}H_{178}O_9$: C, 82.60; H, 9.66. Found: C, 82.68; H, 9.62. MS: m/z, 1859.6 (M^+).

Compound 15a. ^{1}H NMR ($CDCl_3$, ppm): δ 10.25 (s, 1 H), 7.65 (s, 1 H, aromatic H), 7.55 (br, 20 H, aromatic H), 7.51 (s, 1 H, aromatic H), 7.46−7.43 (m, 12 H, aromatic H), 7.42−7.29 (m, 10 H, olefinic H), 7.20 (d, 2 H, aromatic H), 7.18−7.01 (m, 12 H, olefinic H), 3.03 (t, 2 H), 2.77 (m, 18 H), 2.39 (s, 3 H), 1.64 (m, 24 H), 1.29 (m, 120 H), 0.89 (m, 36 H). Anal. Calcd for $C_{192}H_{266}O$: C, 89.03; H, 10.35. Found: C, 88.79; H, 10.28.

Compound 15b. ^{1}H NMR ($CDCl_3$, ppm): δ 10.37 (s, 1 H), 7.48−7.43 (m, 30 H), 7.39−7.36 (dd, 3 H), 7.28 (s, 1 H), 7.13−7.05 (m, 24 H), 4.09 (t, 2 H), 4.03 (m, 22 H), 2.35 (s, 3 H), 1.85 (m, 24 H), 1.51 (m, 24 H), 1.30 (m, 96 H), 0.88 (m, 36 H). Anal. Calcd for $C_{192}H_{266}O_{13}$: C, 82.89; H, 9.66. Found: C, 82.63; H, 9.58. MS: m/z, 2783.1 ($(M + H)^+$).

Preparation of Diblock Copolymers: General Procedure for the Synthesis of Copolymers. The polyisoprene segment was prepared by an anionic living polymerization in moisture and oxygen-free cyclohexane at room temperature, according to ref 43. The aldehyde-terminated OPV was then dissolved in dry and deoxygenated THF by bringing the solution into reflux. After all of the OPV was dissolved, about 0.9 equiv of the living polyisoprene was transferred into the OPV solution through a gastight syringe. At the same time, an aliquot of the polyisoprene solution was terminated with methanol for use in comparison to the diblock copolymer. After 2 h of reaction, the diblock copolymer was precipitated in a 5-fold excess of methanol and coagulated on the bottom of the precipitation flask. Excess solvent and methanol were decanted, and the copolymer was redissolved in $CHCl_3$. Further purification of the copolymer was achieved by flash chroma-

tography using a 1:1 mixture of hexane/chloroform. The diblock copolymer is an orange, rubberlike substance or viscous liquid. All of the copolymers show identical ^{1}H NMR spectra. δ (ppm, $CDCl_3$): 0.89−2.05 (aliphatic protons), 2.77 ($-CH_2-$, next to phenyl ring), 3.75 (CH_3O-), 4.70 (two doublets, 3,4-addition vinyl protons), 5.10 (1,4 addition vinyl proton), 7.55−6.90 (conjugated aromatic and olefinic protons).

Characterization. The ^{1}H NMR spectra were collected on a UC 500 MHz spectrometer. The ^{13}C NMR spectra were obtained using a GE QE 300 MHz spectrometer. The FTIR spectra were recorded on a Nicolet 20 SXB FTIR spectrometer. A Shimadzu UV-2401PC UV−vis recording spectrophotometer and a Shimadzu RF-5301PC spectrofluorophotometer were used to record the absorption and emission spectra. To measure the fluorescence quantum yield, a degassed chloroform solution was prepared. The concentration was adjusted so that the absorbance of the solution would be in the range 0.05−0.1. The exciting wavelength was 360 nm, and 9,10-diphenylanthracene was used as the standard which has a quantum yield of 0.91 in nonpolar solvents. Since the same solvent and exciting wavelength were used for both standard and sample and the solution concentration was so low, solutes would not contribute much to the refractive index of the solution. Both solutions were assumed to have the same refractive index.

The GPC measurements were performed on a Waters RI system equipped with an UV detector, a differential refractometer detector, and Ultrastyragel linear columns at 35 °C using THF (HPLC grade, Aldrich) as the eluent. The molecular weight and molecular weight distribution were calculated on the basis of monodispersed styrene standards. Thermal analyses were collected using the DSC-10 and TGA-50 systems of TA Instruments with a heating rate of 10 °C/min under a nitrogen atmosphere. The polarizing microscopy was performed with a Nikon (OPTIPHOT-2) microscope equipped with a Creative Device 50-600 hot stage. Mass measurements were conducted by Washington University Resource for Biomedical and Bio-organic Mass Spectrometry. The precision for low-resolution FAB experiment is 0.01% (w/w). The precision for MALDI is 0.1% (w/w).

The TEM measurements were performed on a Phillips CM 120 transmission electron microscope operated at 120 kV. Specimens were prepared by spin-casting a 1% solution of the copolymers in toluene onto amorphous silicon nitride substrates at a spinning rate of 3000 rpm. The films were then held under vacuum for 10 h. Samples were examined before and after annealing, which was performed under a constant flow of nitrogen. Annealing temperature and time are usually around 120 °C and 15−20 h. Prior to imaging by TEM, specimens were exposed to osmium tetroxide (OsO_4) vapor for 2 h. OsO_4 preferentially stains the unsaturated bonds of the polyisoprene block, which creates amplitude contrast between the OPV and polyisoprene domains.

Acknowledgment. This work was partially supported by the National Science Foundation and AFOSR. Support from the National Science Foundation Young Investigator program is gratefully acknowledged. This work also benefited from the support of the NSF MRSEC program at the University of Chicago. Assistance on SAXS studies by Professors T. Lodge and F. Bates at University of Minnesota is appreciated.

References and Notes

(1) (a) Skotheim, T. A., Ed. *Handbook of Conducting Polymers*; Marcel Dekker: New York, 1986; Vols. 1 and 2. (b) Skotheim, T. A., Ed. *Electroresponsive Molecular and Polymeric Systems*; Marcel Dekker: New York, 1991; Vol. 2.
(2) Burroughes, J. H.; Bradley, D. D. C.; Brown, A. R.; Marks, R. N.; Mackay, K.; Friend, R. H.; Burn, P. L.; Holmes, A. B. *Nature* **1990**, *347*, 593.
(3) Kiess, H. G., Ed. *Conjugated Conducting Polymers*; Springer Series in Solid State Sciences; Springer-Verlag: Berlin, 1992; p 102.
(4) Henglein, A. *Top. Curr. Chem.* **1988**, *143*, 115.
(5) Steigerwald, M. L.; Brus, L. E. *Annu. Rev. Mater. Sci.* **1989**, *19*, 471.
(6) Wang, Y.; Herron, N. *J. Phys. Chem.* **1991**, *95*, 525.
(7) Chen, X. L.; Jenekhe, S. A. *Macromolecules* **1996**, *29*, 6189.
(8) Widawski, G.; Rawiso, M.; Francois, B. *Nature* **1994**, *369*, 387.
(9) Francois, B.; Pitois, O.; Francois, J. *Adv. Mater.* **1995**, *7*, 1041.
(10) (a) Aldissi, M.; Bishop, A. R. *Polymer* **1985**, *26*, 622. (b) Li, J.; Khan, I. M. *Macromol. Symp.* **1995**, *91*, 141.
(11) Aldissi, M. *J. Chem. Soc., Chem. Commun.* **1984**, 1347.
(12) Saunders, R. S.; Cohen, R. E.; Schrock, R. R. *Macromolecules* **1991**, *24*, 5599.
(13) Sato, M.; Tanaka, S.; Kaeriyama, K. *J. Chem. Soc., Chem. Commun.* **1986**, 873.
(14) Yoshino, K.; Nakajima, S.; Onoda, M.; Sugimoto, R. *Synth. Met.* **1989**, *28*, C349.
(15) Bazan, G. C.; Miao, Y.-J.; Renak, M. L.; Sun, B. J. *J. Am. Chem. Soc.* **1996**, *118*, 2618.
(16) Jenekhe, S. A.; Chen, X. L. *Science* **1998**, *279*, 1903.
(17) Hempenius, M. A.; Langeveld-Voss, B. M. W.; van Haare, J. A. E. H.; Janssen, R. A. J.; Sheiko, S. S.; Spatz, J. P.; Moller, M.; Meijer, E. W. *J. Am. Chem. Soc.* **1998**, *120*, 2798.
(18) (a) Li, W. J.; Maddux, T.; Yu, L. P. *Macromolecules* **1996**, *29*, 7329. (b) Li, W. J.; Maddux, T.; Yu, L. P. *Polym. Prepr.* **1996**, *37*, 378.
(19) Leibler, L. *Macromolecules* **1980**, *13*, 1602.
(20) Hong, K. M.; Noolandi, J. *Macromolecules* **1981**, *14*, 736.
(21) Helfand, E.; Wasserman, Z. R. In *Developments in Block Copolymers*−2; Goodman, I., Ed.; Applied Science Publishers: New York, 1982; pp 99−125.
(22) VanKrevelen, D. W. *Properties of Polymers: Their Estimation and Correlation with Chemical Structure*; Elsevier Scientific Publishing: New York, 1976; p 129.
(23) Maddux, T.; Li, W. J.; Yu, L. P. *J. Am. Chem. Soc.* **1997**, *119*, 844.
(24) Peng, Z.; Gharavi, A.; Yu, L. P. *J. Am. Chem. Soc.* **1997**, *119*, 4623.
(25) Cabri, W.; Candiani, I.; Bedeschi, A.; Santi, R. *J. Org. Chem.* **1992**, *57*, 3558.
(26) Cabri, W.; Candiani, I.; Bedeschi, A.; Santi, R. *Synlett* **1992**, 871.
(27) Richardson, W. S.; Sacher, A. *J. Polym. Sci.* **1953**, *14*, 353.
(28) Allgaier, J.; Poppe, A.; Willner, L.; Richter, D. *Macromolecules* **1997**, *30*, 1582.
(29) Graham, S. C.; Bradley, D. D. C.; Friend, R. H.; Spangler, C. *Synth. Met.* **1991**, 41.
(30) Gartstein, Y. N.; Rice, M. J.; Conwell, E. M. *Phys. Rev. B* **1995**, *52*, 1683.
(31) Bao, Z.; Chen, Y.; Cai, R.; Yu, L. P. *Macromolecules* **1993**, *26*, 5281.
(32) Strey, B. T. *J. Polym. Sci. A3* **1965**, 265.
(33) Seminov, A. N.; Vasilenko, S. V. *Sov. Phys. JETP* **1986**, *63* (1), 70.
(34) Semenov, A. N. *Mol. Cryst. Liq. Cryst.* **1991**, *209*, 191.
(35) Perly, B.; Douy, A.; Gallot, B. *Makromol. Chem.* **1976**, *177*, 2569.
(36) Billot, J.-P.; Douy, A.; Gallot, B. *Makromol. Chem.* **1977**, *178*, 1641.
(37) Bates, F. S.; Rosedale, J. H.; Fredrickson, G. H. *J. Chem. Phys.* **1990**, *92*, 6255.
(38) Sakamoto, N.; Hashinoto, T. *Macromolecules* **1995**, *28*, 6825.
(39) Sakamoto, N.; Hashinoto, T. *Macromolecules* **1996**, *29*, 8126.
(40) Mortensen, K.; Brown, W.; Almdal, K.; Alami, E.; Jada, A. *Langmuir* **1997**, *13*, 3635.
(41) Kitazume, T.; Lin, J. T.; Takeda, M.; Yamazaki, T. *J. Am. Chem. Soc.* **1991**, *113*, 2123.
(42) Peters, M. A.; Belu, A. M.; Linton, R. W.; Dupray, L.; Meyer, T. J.; DeSimone, J. M. *J. Am. Chem. Soc.* **1995**, *117*, 3380.

MA981679I